Unraveling the mechanisms behind the complete suppression of cocaine electrochemical signals by chlorpromazine, promethazine, procaine, and dextromethorphan

Article

Unraveling the mechanisms behind the complete suppression of cocaine electrochemical signals by chlorpromazine, promethazine, procaine and dextromethorphan

Mats de Jong, Nick Sleegers, Anca Florea, Joren Van Loon, Alexander L.N. van Nuijs, Nele Samyn, and Karolien De Wael

Anal. Chem., **Just Accepted Manuscript** • DOI: 10.1021/acs.analchem.9b03128 • Publication Date (Web): 14 Nov 2019

Unraveling the mechanisms behind the complete suppression of cocaine electrochemical signals by chlorpromazine, promethazine, procaine and dextromethorphan

Mats de Jong[a], Nick Sleegers[a], Anca Florea[a], Joren Van Loon[a,b], Alexander L. N. van Nuijs[c], Nele Samyn[d], and Karolien De Wael[a]*

[a]AXES Research Group, University of Antwerp, Groenenborgerlaan 171, 2020 Antwerp, Belgium

[b]Product Development Research Group, University of Antwerp, Ambtmanstraat 1, 2000 Antwerp, Belgium

[c]Toxicological Center, University of Antwerp, Universiteitsplein 1, 2610 Antwerp, Belgium

[d]Drugs and Toxicology Department, National Institute for Criminalistics and Criminology, Vilvoordsesteenweg 100, 1120 Brussels, Belgium

*E-mail: Karolien.DeWael@uantwerpen.be.

ABSTRACT: The present work investigates the challenges accompanied with the electrochemical cocaine detection in physiological conditions (pH 7) in the presence of chlorpromazine, promethazine, procaine and dextromethorphan, frequently used cutting agents in cocaine street samples. The problem translates into the absence of the cocaine oxidation signal (signal suppression) when in mixture with one of these compounds, leading to false negative results. Although a solution to this problem was provided through earlier experiments of our group, the mechanisms behind the suppression are now fundamentally investigated via electrochemical and liquid chromatography quadrupole-time-of-flight mass spectrometry (LC-QTOF-MS) strategies. The latter was used to confirm the passivation of the electrodes due to their interaction with promethazine and chlorpromazine. Electron transfer mechanisms were further identified via linear sweep voltammetry. Next, adsorption experiments were performed on the graphite screen printed electrodes both with and without potential assistance in order to confirm if the suppression of the cocaine signals is due to passivation induced by the cutting agents or their oxidized products. The proposed strategies allowed to identify the mechanisms of cocaine suppression for each cutting agent mentioned. Suppression due to procaine and dextromethorphan is caused by fouling of the electrode surface by their oxidized forms, while for chlorpromazine and promethazine the suppression of the cocaine signal is related to the strong adsorption of these (non-oxidized) cutting agents onto the graphite electrode surface. These findings provide fundamental insights in possible suppression and other interfering mechanisms using electrochemistry in general, not only in the drug detection sector.

Drugs of abuse production, trafficking and consumption are becoming a globally greater issue year by year. It is estimated by the United Nations Office on Drugs and Crime (UNODC) that 275 million people used drugs in 2016, counting for an increase of 32% compared to the situation in 2006. Also, the production of drugs has increased, as well as the number of global seizures. More alarmingly, the amount of global deaths directly caused by the use of drugs (mainly opioids and, more recently, also fentanyl and derivatives) has been continuously increasing the last two decades from approximately 105,000 deaths in 2000 to 168,000 deaths in 2015, which is an increase of 60%.[1]

Cocaine is a stimulant drug which is highly addictive and harmful for people's health. On short-term basis, undesirable effects like an increased heart rate, blood pressure and respiration rate could occur, while after long-term use the addiction might cause a state of lethargy, extreme tiredness and depression when the cocaine consumption stops.[2-5]

Today, cocaine is the most seized illicit drug in North America, South America and Europe, apart from cannabis, in measure of total weight.[1, 6-7] In 2016, just over 1,100 tons of cocaine have been seized, which is an increase of 67% compared to 2014. These findings are also supported by the numbers of global coca bush cultivation area and cocaine production, showing an increase of 60% to 213,000 hectares and an increase of 50% cocaine produced to 1,410 tons, respectively, over the same time period.[1] In Oceania, Asia and Africa, the share of cocaine seizures is less significant.[1, 8-9]

The development of fast and reliable methods for cocaine detection is of great importance for public authorities to tackle the problem of drug trafficking, production and consumption. Current field tests in the form of color tests (e.g. Scott test for cocaine) are cheap and easy to use, but lack specificity and are easily bypassed by adding coloring agents.[10-13] Specificity is crucial because cocaine samples are usually adulterated with other, legal, compounds, mimicking the stimulating effects of cocaine or used as fillers to maximize profit. In general, these compounds are described by the term cutting agents. Sometimes, cutting agents produce the same color in the test as cocaine, leading to unjustified seizures of cargo and detention of innocent people.[11] After performing a presumptive test, confirmation is required by chromatographic separation

coupled to mass spectrometry. These methods are laborious in use, expensive, and hardly portable.[3, 10] Electrochemical techniques offer a good alternative for on-site screening of illicit drugs because of their simplicity, low cost, robustness, fast response and high sensitivity. Moreover, compared to spectrometry-based techniques, electrochemical instrumentation can be miniaturized to the size of a smartphone, and even smaller. Using disposable screen printed electrodes (SPE) allows fast analysis for multiple samples.

Electrochemical detection of cocaine and other narcotics and cutting agents is the topic of several works, in which mostly modified electrodes or deconvolution methods are needed for the identification. This leads to a time consuming and costly approach in screening settings.[14-20] In our previous work, the use of electrochemistry showed a great advantage over the use of classical color tests for the on-site screening of cocaine.[11] Additionally, selectivity could be achieved by optimizing electrochemical strategies, without electrode modification or extensive software methods. This work has shown that pH influences the resolution of the redox peaks. At pH7, the electrochemical cocaine signal was completely suppressed when cocaine was mixed with chlorpromazine, promethazine, levamisole, procaine or dextromethorphan. This leads to a false negative result in a screening test. Alternatively, a cathodic pretreatment of the electrode surface aided the detection of cocaine in the presence of levamisole in physiological conditions.[21] More recently, Florea *et al.* provided suitable polymer platforms, also allowing detection of cocaine in the presence of levamisole.[22]

Although a solution for the suppression caused by the aforementioned compounds was provided in our earlier work, the mechanisms causing this suppression were not studied yet.[11, 21] In this work, we present our findings and unravel the mechanism behind, meanwhile delivering valuable generic information on the prevention of suppression of electrochemical signals by interfering compounds.

Several mechanisms of suppression could be expected from mechanistically related problems and are shown in Figure 1: (A) inhibition by the presence of a matrix compound that strongly adsorbs to the working electrode surface, hindering the access of the analyte of interest, here cocaine, to the surface, preventing the occurrence of an analyte-related electron transfer; (B) inhibition caused by fouling of the electrode due to the presence of created oxidation products of a matrix compound, which strongly interact with the electrode surface, preventing an analyte-related electron transfer. A special case of (B) is electropolymerization, where a matrix compound polymerizes during electrochemical processes to form a film on the electrode surface, either aiding or inhibiting the electron transfer[22]; (C) inhibition by a fast chemical reaction occurring between the analyte and either a matrix compound or (D) an oxidized matrix compound, leading to a sudden concentration drop of the analyte, making it undetectable. Complexation of the analyte with a matrix compound is not considered since this phenomenon typically results in a potential shift of the voltammetric signal of the analyte, rather than a complete suppression of the signal.[11, 23]

In this article, the suppression effects of given cutting agents on the electrochemical oxidation of cocaine will be illustrated. Next, the nature of the electrode process (i.e. diffusion or adsorption control) will be determined for all interfering compounds, giving the general idea what type of suppression mechanisms might occur. Then, MS approaches are utilized to study if the adsorption control compounds lead to a physical blockage of the electrode surface. In addition, voltammetry and MS approaches are utilized to study if any of the compounds lead to a physical blockage of the electrode surface via adsorption. Finally, voltammetry and electrochemical impedance spectroscopy are selected to study the influence of oxidized matrix compounds on the electrochemical signal of cocaine and on the blockage of the electrode surface.

EXPERIMENTAL SECTION

Reagents and Samples

Cocaine HCl (COC) standards were purchased from Lipomed (Arlesheim, Switzerland). Standards of dextromethorphan HBr (DXM), procaine HCl (PRC) and norcocaine (NC) were purchased from Sigma-Aldrich (Diegem, Belgium). Standards of promethazine HCl (PMZ) and chlorpromazine HCl (CPMZ) were purchased from TCI Chemicals (Zwijndrecht, Belgium).

$K_3Fe(CN)_6$, $K_4Fe(CN)_6$, potassium monophosphate, potassium chloride and potassium hydroxide were purchased from Sigma-Aldrich (Diegem, Belgium). A solution of 20 mM phosphate buffer containing 100 mM KCl was used as supporting electrolyte and the pH was adjusted to 7 using a 100 mM KOH solution with a CyberScan 510 pH-meter from Eutech Instruments (Landsmeer, The Netherlands) connected to

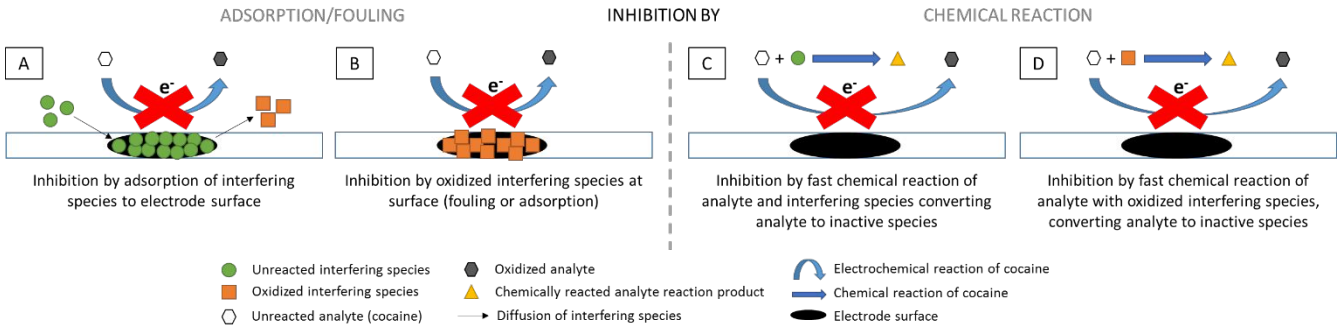

Figure 1. Possible mechanisms of voltammetric signal suppression: adsorption of either the interfering (A) or oxidized interfering species (B); chemical reaction of analyte with either the interfering (C) or oxidized interfering species (D).

a HI-1131 glass bodied pH electrode from Hanna Instruments (Bedfordshire, United Kingdom). All aqueous solutions were prepared using double distilled water. The reagents were of analytical grade and used without further purification.

Instrumentation and apparatus

Electrochemical measurements, including square wave voltammetry (SWV), linear sweep voltammetry (LSV) and cyclic voltammetry (CV), were carried out with an Autolab potentiostat/galvanostat (PGSTAT 302N, Metrohm, Switzerland) controlled by NOVA 2.1 software.

Disposable carbon ItalSens IS-C Screen Printed Electrodes (SPE) were purchased from PalmSens (Utrecht, The Netherlands) and were used during all electrochemical measurements. The SPE's contain an internal silver pseudo reference electrode and a carbon counter electrode.

All experiments were performed by applying 50 µL of solution onto the SPE. All SWV measurements were carried out with a step potential of 5 mV, amplitude of 25 mV and frequency of 10 Hz. All results obtained by SWV were presented after baseline correction using the mathematical algorithm "moving average" (peak width = 1) contained within NOVA 2.1 software, which improves the visualization and identification of the peaks over the baseline. All electrochemical experiments were performed at room temperature.

All LSV measurements were performed using a step potential of 5 mV and varying the scan rate from 5 to 500 mV s^{-1}.

Electrochemical impedance spectroscopy (EIS) experiments were performed using a sine potential wave varying to 40 different frequencies in the range of 100 000 – 0.1 Hz (logarithmic steps) and an amplitude of 10 mV. A 5 mM $K_3Fe(CN)_6$ and $K_4Fe(CN)_6$ solution was used to determine the charge transfer resistance R_{CT} by fitting the data to the $[R_S(Q[R_{CT}W])]$ scheme, the so-called Randles Circuit, in a Nyquist plot. In this scheme, R_S stands for the electrolyte resistance, Q for the constant phase element, which is in an ideal case a capacitor related to the electric double layer capacitance, and W for the Warburg element, accounting for mass transport.

All electrochemical experiments were performed using 20 mM KH_2PO_4 pH 7 buffer containing 100 mM KCl as an electrolyte.

Mass spectra were recorded using LC coupled to a QTOF-MS mass spectrometer with electrospray ionization (ESI) operating in positive mode. The apparatus consisted of a 1290 Infinity LC (Agilent Technologies, Wilmington, DE, USA) connected to a 6530 Accurate-Mass QTOF-MS (Agilent Technologies) with a heated-ESI source (JetStream ESI). Chromatographic separation was performed on a Kinetex Biphenyl column (150 × 2.1 mm, 2.6 µm), maintained at room temperature, and using a mobile phase composed of 0.04% of formic acid in ultrapure water (A) and acetonitrile/ultrapure water (80/20, v/v) with 0.04% formic acid (B), in gradient. The flow rate and the injection volume were set at 0.3 mL/min and 1 µL, respectively. The QTOF-MS instrument was operated in the 2 GHz (extended dynamic range) mode, which provides a full width at half maximum (FWHM) resolution of approximately 4700 at *m/z* 118 and 10,000 at *m/z* 922. Positive polarity ESI mode was used under the following specific conditions: gas temperature 300 °C; gas flow 8 L/min; nebulizer pressure 40 psi; sheath gas temperature 350 °C; sheath gas flow 11 L/min. Capillary and fragmentor voltages were set to 4000 and 135 V, respectively. A reference calibration solution (provided by Agilent Technologies) was continuously sprayed into the ESI source of the QTOF-MS system. The ions selected for recalibrating the mass axis, ensuring the mass accuracy throughout the run were *m/z* 121.0508 and 922.0097 for positive mode. The QTOF-MS device was acquiring from *m/z* 50 to 1000 in MS mode. Data-dependent acquisition mode (auto-MS/MS) was applied using two different collision energies (10 and 20 eV) for the fragmentation of the selected parent ions. The maximum number of precursors per MS cycle was set to four with minimal abundance of 2500 counts. In addition, precursor ions were excluded after every spectrum and released after 0.2 min.

RESULTS AND DISCUSSION

Challenges with cocaine detection at pH 7

Although electrochemical detection of COC in the presence of PRC, DXM, PMZ and CPMZ is possible in alkaline conditions, it was previously demonstrated that suppression effects occur at pH 7.[11] This poses a problem for on-site COC detection in powders, but also in human samples. Although the detection in humans is not within the scope of this work, it is important to know why the detection of COC is hampered at pH 7 for future applications and generic understanding. This will eventually lead to a deep understanding of the electrochemical fingerprints and motivates our work laying the basis for the development of robust sensors. The chemical structures of the relevant compounds are shown in Figure 2.

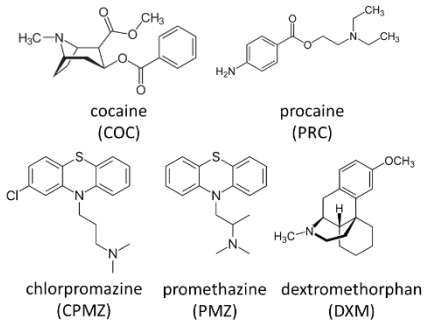

Figure 2. Chemical structures of COC and the four compounds causing electrochemical suppression of COC: PRC, CPMZ, PMZ and DXM.

Figure 3 illustrates the suppression effect of PMZ, PRC, DXM and CPMZ on COC detection. Whilst a pure COC solution in pH 7 buffer shows a clear signal at 1.03 V in the SWV, the binary mixtures with a molar ratio of 1:1 COC:cutting agent do not. The presence of COC is completely suppressed, leading to a false negative result, while the original signals of CPMZ, PMZ, PRC and DXM are still visible in these voltammograms (voltammograms of pure compounds in Figure S-1 of the *Supporting Information*). This observation makes mechanisms C and D of Figure 1 unlikely to occur, as in that case the other signals should also lose a significant amount of intensity. Moreover, the chemical reaction would need to be extremely fast (time scale of voltammetry experiment is seconds).

Electropolymerization of matrix compounds onto the electrode surface can be ruled out. Electropolymerization typically requires the application of multiple voltammetry scans in optimized conditions using pre-modified electrodes in order to allow significant polymerization to occur at the electrode surface. Therefore, it is unlikely to occur as an inhibition factor in a single sweep voltammetry experiment on an unmodified electrode.[22]

A systematic approach is now implemented to determine the suppression mechanism (i.e. mechanism A, B, C or D from Figure 1) for each cutting agent by means of electrochemical techniques and liquid chromatography-mass spectrometry.

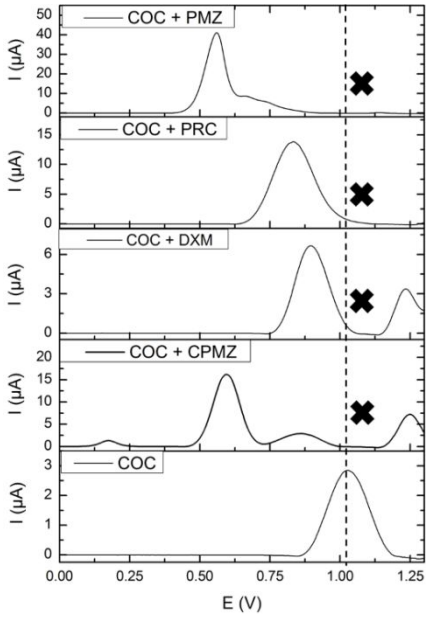

Figure 3. SWVs of COC (0.5 mM) and binary mixtures (1:1) of COC (0.5 mM) and suppressing agents (0.5 mM) for interfering agents PMZ, PRC, DXM and CPMZ in pH 7. The black dashed straight line indicates where the COC signal should be present. The crosses indicate the absence of the COC signal.

Electrode processes

PMZ and CPMZ are closely related phenothiazine derivatives characterized by their triple ring core structure (Figure 2). This planar core structure has a hydrophobic character and could therefore interact significantly with the carbon working electrode surface. This might cause strong adsorption phenomena of both compounds onto these electrodes, influencing their oxidation processes as well as that of other compounds present in a mixture.[24-25] Therefore, it is expected that the presence of a significant amount of PMZ or CPMZ blocks or passivates the electrode surface, hindering the electron transfer of COC-related oxidation processes, as is projected in Figure 1A. PRC is an aminobenzoate which is more hydrophilic compared to CPMZ and PMZ. Therefore, a diffusion controlled oxidation mechanism is more likely to take place as is the case for DXM, which also has more hydrophilic properties compared to CPMZ and PMZ.

These hypotheses were confirmed by performing LSV on solutions containing either PMZ, CPMZ, PRC or DXM (0.5 mM), with varying scan rate (5-10-20-50-100-200-500 mV s^{-1}). The results are shown in Figure S-2 in the *Supporting Information*. In both the case of PMZ and CPMZ, a linear relation is observed for the measured peak current (I_P) and the applied scan rate (ν) (R^2 = 0.997 and 0.998, respectively), while the I_P vs $(\nu)^{1/2}$ plot is not linear (R^2 = 0.957 and 0.919, respectively). Therefore, an adsorption controlled mechanism is taking place, in relation to the hydrophobic character of PMZ, CPMZ and the electrode surface.[25] For PRC, the I_P vs. $\nu^{1/2}$ plot is linear (R^2 = 0.9997). This implies a diffusion controlled process, similar as for DXM (R^2 = 0.996).

With this knowledge, mechanism A from Figure 1 could indeed be appointed as the most likely mechanism of suppression of COC by PMZ and CPMZ, while mechanism A can most likely be ruled out for PRC and DXM. Further gathering of evidence is, however, necessary.

Exclusion of mechanisms C and D for PMZ, CPMZ, PRC, DXM

The exclusion of mechanism C and D and thus passivation of the electrode surface, induced by its interaction with a mixture of COC and PMZ or CPMZ, is evidenced by performing electrolysis and LC-QTOF-MS. An electrolysis of 1 hour was performed at a potential of 1 V with a pure 200 µM solution of COC and a mixture of 200:200 µM COC:PMZ in a small electrolysis cell containing 200 µL solution dropped on the SPE. It was determined in earlier research that during oxidation of COC, an imine is mainly formed from the tertiary amine, which is then easily and almost immediately rearranged in aqueous media to NC (a secondary amine) and formaldehyde.[14, 26] NC is therefore the main oxidation product of COC. The amount of NC formed during electrolysis will be therefore significantly higher at a non-passivated electrode compared to a physically blocked electrode surface.

The LC analysis of an electrolyzed COC solution (1 hour) (Figure 4, dashed line) clearly illustrates the formation of NC (retention time 5.5 minutes) (Figure 4, dotted line). The product corresponding with this signal was investigated further with MS/MS to obtain the fragmentation pattern (inset Figure 4) and this pattern shows next to the parent ion at *m/z* 290 two fragments at *m/z* 136 and 168, typical for NC. In contrast to the chromatograms obtained for pure COC after electrolysis and pure NC, the third chromatogram in Figure 4 (solid line) corresponds to the mixture of COC and PMZ after electrolysis. It hardly shows any formation of NC as oxidation product of COC, proving that the electron transfer is hindered and the electrode passivated. Therefore, the occurrence of suppression mechanisms C and D from Figure 1 is ruled out for COC suppression by CPMZ and PMZ.

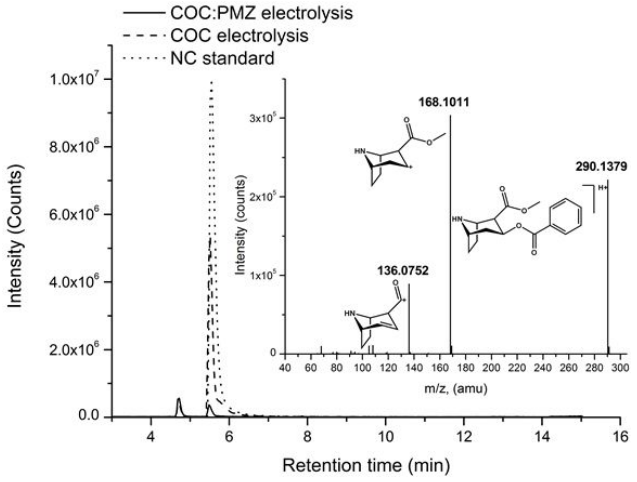

Figure 4. LC chromatogram of a 200 µM NC standard (dotted line), a 200 µM COC standard after 1h electrolysis (dashed line), and a 200:200 µM COC:PMZ solution after 1h electrolysis (solid line). Inset: MS/MS fragmentation data of NC.

Concerning PRC and DXM, the physical blockage of the electrode is further evidenced by performing EIS with a 5:5 mM $K_3Fe(CN)_6$: $K_4Fe(CN)_6$ solution prior to and after SWV potential sweeps with PRC and DXM (0 - 1.3 V). Between every EIS and SWV step, the electrode was rinsed. The charge transfer resistance (R_{CT}) is derived from the measured Nyquist plots which were fitted to the Randles [$R_S(Q[R_{CT}W])$] scheme. The R_{CT} can be interpreted in Figure S-3 (*Supporting Information*) from the diameter of the semi circles. After fitting, the R_{CT} for the blank, after 1, 2 and 3 SWV scans with 0.5 mM PRC or DXM were found to be 102, 965, 4190 and 5130 Ω for PRC and 329, 893, 1840 and 2240 Ω for DXM, respectively. The increasing R_{CT} with the number of SWV sweeps with PRC or DXM delivers a convincing indication that the electrodes become physically blocked during the oxidation sweep. This indicates another suppression mechanism than C or D is at work for COC suppression.

Confirmation or exclusion of mechanism A

In order to determine whether the adsorption of the matrix compound onto the electrode surface (suppression mechanism A) is the only reason for a suppressed COC signal, one has to confirm if this adsorption leads to a complete blockage of the electrode surface, disallowing electron transfer of other present compounds (such as COC) which typically undergo diffusion controlled reactions. Therefore, solutions containing different concentrations of PMZ, CPMZ, PRC or DXM were dropped on the electrode surface and incubated for one minute without applying a potential, after which the solution was removed, the electrodes rinsed and a new solution containing 0.5 mM COC was analyzed with SWV. The same experiment was performed with a fixed concentration (0.5 mM) of PMZ, CPMZ, PRC or DXM, where in this case the incubation time was varied. The SWVs were compared to the ones of pure COC and pure PMZ, CPMZ, PRC and DXM at a non-treated electrode surface. The results are shown in Figure 5. Figure 5A, C, E and G, respectively show the influence of increasing PMZ, CPMZ, PRC and DXM concentration during the incubation step on the SWV of the later added 0.5 mM COC solution. Figures 5B, D, F and H show the influence of increasing the incubation time. Two pieces of data from these figures will be used to prove or exclude suppression mechanism A from Figure 1: (1) the loss of intensity of the COC signal or total absence of it; and (2) the presence of clear signals of the suppressing compound.

Suppression mechanism A from Figure 1 can be ruled out as a possible mechanism for PRC and DXM. Neither by increasing the concentration in the incubation step nor by increasing the incubation time, the COC signal loses intensity. In addition, the absence of clear PRC and DXM signals in the SWV (typically at 0.65 V) makes mechanism A impossible. Impedance data emphasizes these findings even further as EIS was performed after incubation and rinsing of the electrode using the $Fe(CN)_6^{3-/4-}$ redox couple. The electron transfer resistance is not influenced by the incubation of PRC or DXM (Figure S-4 in *Supporting Information*), once again excluding the possibility of PRC and DXM adsorbing at the surface, blocking it.

PMZ and CPMZ on the other hand are adsorbed at the electrode surface after rinsing the electrode since their characteristic SWV signals (maxima at ca. 0.50 V and 0.70 V for PMZ and ca. 0.65 V and 0.85 V for CPMZ) are still visible with a high current intensity in the SWV of the later measured COC solution. It is clear that a higher concentration during incubation results in a higher amount of adsorbed PMZ or CPMZ onto the electrode surface, as is shown by the increasing intensity of the respective signals with concentration. A significant increase in intensity is observed when going from 1 mM to 2 mM incubation, indicating that somewhere between these concentrations, the adsorption of PMZ onto the electrode surface becomes much more prominent. Increasing the incubation time only results in a limited increase of the PMZ and CPMZ signal intensity. The COC SWV signal is completely suppressed after incubation with CPMZ in all different conditions, apart from 1 minute incubation with 0.5 mM CPMZ (3% of the COC signal intensity remains in this case). The CPMZ data is shown in Figure 5C + inset and D. This is not the case for PMZ. In analogy to the signal of PMZ, the COC signal becomes fully suppressed when the transition is made from incubation with 1 mM to 2 mM PMZ.

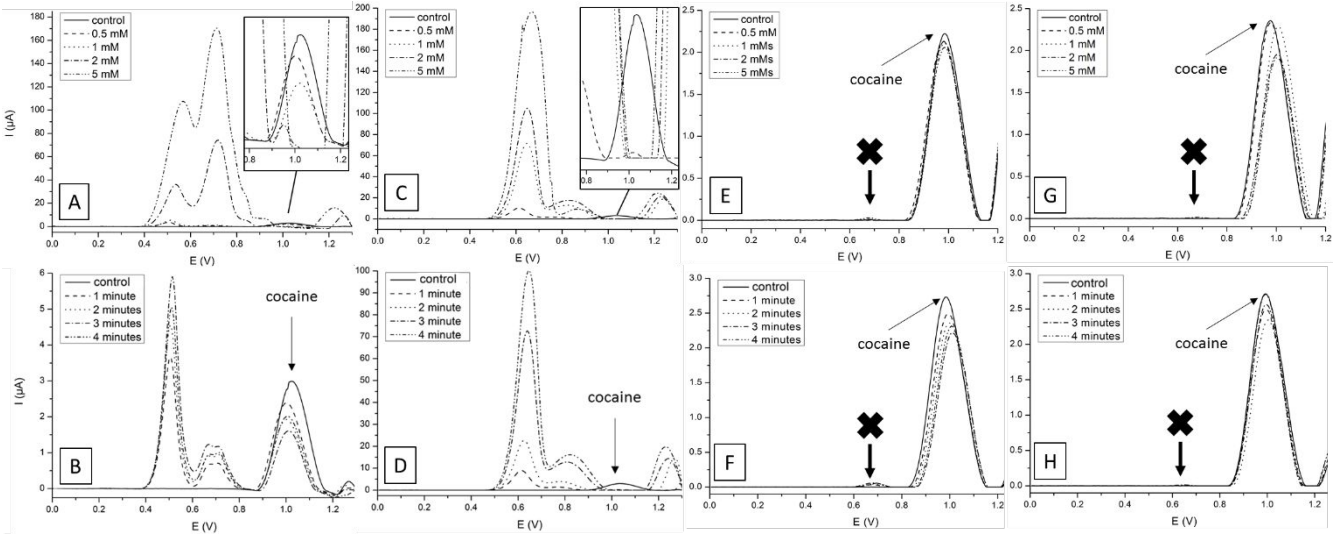

Figure 5. SWV recordings of 0.5 mM COC after 1 minute of incubation with either 0.5, 1, 2 or 5 mM solution of PMZ (A), CPMZ (C), PRC (E) and DXM (G). SWV recordings of 0.5 mM COC after incubation with 0.5 mM solution of PMZ (B), CPMZ (D), PRC (F) or DXM (H) for 1, 2, 3 and 4 minutes. A curve for COC without incubation is shown as a reference (control).

These combined findings make suppression mechanism A for CPMZ a certainty, but some doubt concerning the mechanism of PMZ still occurs. Although the PMZ signal itself is clearly present, the data from Figure 5A and B show the COC signal is not fully suppressed at any point using 0.5 mM as concentration, which is the concentration PMZ used in our problem definition. The real concentration of PMZ and CPMZ required for total blockage of the electrode (and to prevent the COC electron transfer) could in fact be significantly lower for the following reasons: (1) the rinsing step after the incubation step removes a considerable portion of the adsorbed PMZ and CPMZ from the electrode surface prior to measurement, allowing the electron transfer to occur, whereas these compounds do block the surface completely when directly measured in a mixture with COC; (2) next to the adsorption phenomena described above, applying potentials at the electrode surface might also influence those phenomena along potential sweeps. Applying a positive potential attracts extra PMZ and CPMZ molecules to the formed electrical double layer via diffusion from the bulk, increasing the adsorption effect onto the electrode surface, leading to full COC suppression in SWV with lower concentrations of PMZ and CPMZ than 0.5 mM.

More evidence to allocate suppression mechanism A to PMZ is acquired by performing CV for five consecutive scans, showing that the oxidation signal of PMZ does not lose intensity in function of scan number (Figure S-5 in *Supporting Information*). The oxidation of PMZ is an irreversible process, which implies that the oxidized PMZ should continuously be removed by fresh PMZ from the solution as is shown in Figure 1A.[27-28] This could only be the case if the oxidized product is considerably less hydrophobic compared to PMZ. It is reported that the oxidation process is related to the oxidation of the core phenothiazine ring in two steps to the corresponding, less hydrophobic, sulfoxide.[28-29] Two electrons and two protons are exchanged in the process.

LC-QTOF measurements after 1 hour of electrolysis at a potential of 1 V were performed in order to confirm the formation of mainly the corresponding sulfoxide compound. This product has, in correspondence to the much lower retention time in the LC data (Figure 6, compound 1), a significantly higher polarity compared to PMZ itself, confirming the hypothesis that the much more hydrophobic PMZ is displacing the oxidized sulfoxide from the electrode surface because it interacts stronger with it.

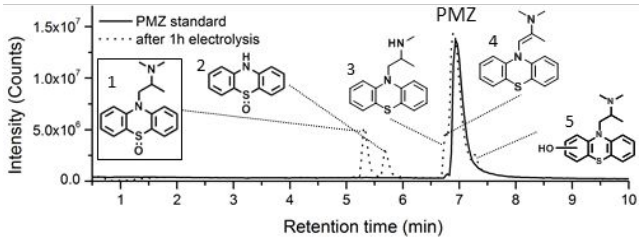

Figure 6. Chromatogram of a 200 μM PMZ standard (solid line) and a 200 μM PMZ standard after 1h electrolysis (dotted line), with oxidation products indicated. Numbers 1 to 5 indicate the different compounds formed during electrolysis. The bordered structure is the main compound formed.

Next to this sulfoxide, four other minor oxidation compounds are formed (2-5 in Figure 6). All oxidation products were identified using MS/MS (data of fragmentation patterns not shown). The proposed complete oxidation mechanism is shown in Figure S-6 of the *Supporting Information*. An analogue mechanism is taking place for CPMZ.

All these findings confirm that mechanism A is indeed the suppression mechanism for PMZ and CPMZ.

Confirmation or exclusion of mechanism B

As suppression mechanisms A, C and D have already been proven impossible for PRC and DXM, the confirmation of mechanism B, i.e. the adsorption of or electrode fouling by their oxidation products, was the remaining goal. In order to confirm this, multiple SWV potential sweeps were performed with 0.5 mM PRC or DXM. The electrodes were rinsed after each sweep. The resulting voltammograms are shown in Figure 7.

The first important observation is made when looking at four consecutive SWV scans of a 0.5 mM PRC or DXM solution. The SWVs show a decrease of the peak current after each scan, demonstrating the formation of oxidation products on the electrode surface, causing fouling which influences the oxidation process of the compounds in the next scan. In addition, a measurement of 0.5 mM COC solution was performed after the SWV's with PRC and DXM and the impact on the COC peak current registered. The results are shown in Figure 8. The effect of varying the end potentials was also studied, in the case of PRC 1.3, 1.0, 0.6 and 0.4 V, in the case of DXM 1.3, 0.7 and 0.4 V.

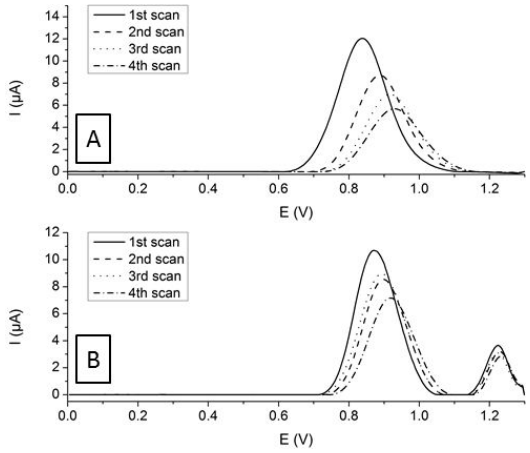

Figure 7. SWV of consecutive scans of (A) 0.5 mM PRC and (B) 0.5 mM DXM solution.

It is immediately clear from Figure 8A that a significant decrease in COC peak current intensity takes place when potential sweeps up to 1.3 and 1.0 V are applied to 0.5 mM PRC solutions prior to the COC SWV. The COC current intensity drops to approximately 4% and 7% of their initial values after one sweep with PRC for these respective potentials and drops further to zero when multiple PRC potential sweeps are performed. Such a drastic effect is not visible when potentials up to 0.6 and 0.4 V were applied in the SWV (55% and 83% of COC current intensity remain after one scan, respectively). A similar trend is observed for DXM (Figure 8B), albeit less noticeable than for PRC, with a drop of the COC signal to 67% of the initial value after one sweep to 1.3 V, slightly above 30% after two and three sweeps until approximately 25% after four sweeps with DXM. If 0.7 V is chosen as upper potential for the DXM sweeps, which is slightly lower than its oxidation potential, the decrease in COC current is only marginal. The COC peak current retains 83% of its initial value after one sweep and drops only slightly further to approximately 75% after four potential sweeps. Oxidation of DXM might still occur slightly at this potential since it is so close to its onset oxidation potential. If we move to an upper potential removed even further from the oxidation peak potential of DXM, the decrease is not even observed and the measured current for COC remains the same after each sweep with DXM. The corresponding SWV's of the COC measurements related to Figure 8 are shown in Figure S-7 of the *Supporting Information*.

These findings for PRC and DXM, in combination with the results of the previous section, and the earlier obtained EIS data from Figure S-3 deliver proof that oxidation products of PRC and DXM are fouling the electrode surface, preventing the detection of COC. Thus, suppression mechanism B of Figure 1 occurs. The fact that for upper potentials 0.6 and 0.4 V for PRC and 0.7 and 0.4 V for DXM the afterward measured COC current does not drop further when multiple SWV sweeps were performed also supports this theory, because at these potentials none (or very limited) of the PRC and DXM should have oxidized.

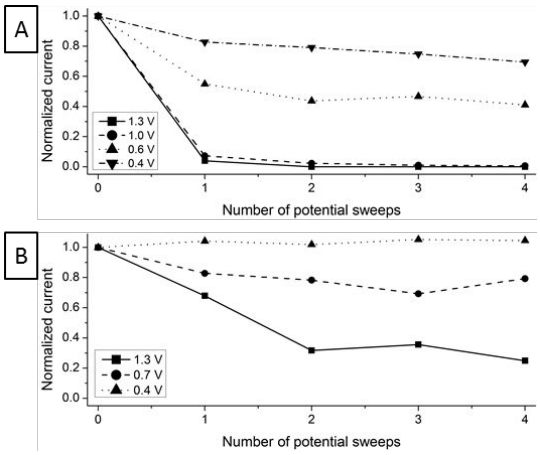

Figure 8. Normalized currents for COC in a recorded SWV (0.5 mM) after 0, 1, 2, 3 and 4 previously performed potential sweeps with (A) 0.5 mM PRC until an upper potential of 1.3 (square), 1.0 (circle), 0.6 (upward triangle) and 0.4 V (downward triangle) and (B) 0.5 mM PRC until an upper potential of 1.3 (square), 0.7 (circle) and 0.4 V (upward triangle).

CONCLUSION

The suppression of the electrochemical oxidation signal of COC in the presence of PRC, DXM, CPMZ and PMZ at graphite SPE's at pH 7 represents a problem for the screening of COC samples containing one of these compounds, leading to false negative results. The fundamental mechanisms behind the suppression are now clarified.

We demonstrated the usefulness of voltammetry, liquid chromatography mass spectrometry and electrochemical impedance spectroscopy in order to unravel the mechanisms behind the suppression phenomena in voltammetry. These measurements were carried out on binary mixtures of COC with either PRC, DXM, CPMZ or PMZ and showed that the origin of the suppression effect is different for the various compounds. For CPMZ and PMZ, the interference is related to the strong adsorption of those two compounds, prior to oxidation, onto the electrode surface, blocking the surface for the COC-related electron transfer, and thus hindering the detection of COC. This was proven by incubation of the electrode with solutions of different concentrations of one of these compounds, after which a COC SWV was performed. A second approach with LC-QTOF-MS indicated that a sulfoxide was formed as main oxidation product of PMZ, which was found to be much less hydrophobic, also indicating PMZ and CPMZ are passivating the electrode surface and not their oxidation products. For PRC and DXM, the suppression of the COC signal is accounted to the respective electrochemical processes at the electrode surface, leading to the adsorption of oxidation products and electrode fouling. These oxidation products prevent the electron

transfer of COC taking place, leading to a false negative result for COC detection. This was evidenced by SWV measurements performed on PRC and DXM solutions up to different upper potentials, after which a SWV was performed on the same electrode with a COC solution. Complementary evidence was delivered by performing the same SWV measurements with PRC and DXM after which EIS was performed, showing an increasing R_{CT} after 1, 2 or 3 SWV scans with PRC or DXM.

With this gained knowledge, actions can be taken in order to further improve voltammetric detection methods, preventing interference by compounds to prevent false negative results.

ASSOCIATED CONTENT

Supporting Information

The Supporting Information is available free of charge on the ACS Publications website.

Electrochemical fingerprints of COC, PMZ, PRC, DXM and CPMZ; scan rate studies (LSV) with PMZ, CPMZ, PRC and DXM; EIS after incubation and oxidation with PRC and DXM; incubation experiments with PRC and DXM (EIS); consecutive CV scans of PMZ; oxidation mechanism of PMZ; SWV potential variation studies of PRC and DXM.

AUTHOR INFORMATION

Corresponding Author

*E-mail: Karolien.DeWael@uantwerpen.be.

Author Contributions

All authors have approved the final version of the manuscript.

ACKNOWLEDGMENT

The authors acknowledge financial support from IOF-SBO/POC (UAntwerp) and the Fund for Scientific Research (FWO) Flanders, Grant 1S 37658 17N.

REFERENCES

(1) United Nations Office on Drugs and Crime (UNODC). *World drug report 2018*, United Nations Publication: Vienna, Austria, 2018. https://www.unodc.org/wdr2018/, (accessed 5th of March 2019).

(2) Samyn, N.; Wille, S.; de Boeck, G., *Handboek forensisch onderzoek*. Uitgeverij Politeia: Brussels, 2009.

(3) United Nations Office on Drugs and Crime. *Recommended methods for the Identification and Analysis of Cocaine in Seized Materials*, New York, USA, 2012. https://www.unodc.org/documents/scientific/Cocaine_Manual_Rev_1.pdf, (accessed 5th of March 2019).

(4) Wunsch, H. *Lancet* **1999**, *353*, 1943.

(5) Missouris, C. G.; Swift, P. A.; Singer, D. R. J. *Lancet* **2001**, *357*, 1586.

(6) European Monitoring Center for Drugs and Drug Addiction. *European Drug Report 2018*, Lisbon, Portugal, 2018. http://www.emcdda.europa.eu/edr2018_en, (accessed 5th of March 2019).

(7) U.S. Customs and Border Protection. *CBP Enforcement Statistics FY2018*, U.S. Department of Homeland Security: 2018. https://www.cbp.gov/newsroom/stats/cbp-enforcement-statistics, (accessed 5th of March 2019).

(8) Australian Criminal Intelligence Commission. *Illicit Drug Data Report 2016-17*, 2018. https://www.acic.gov.au/publications/intelligence-products/illicit-drug-data-report-2016-17, (accessed 5th of March 2019).

(9) Kanato, M.; Choomwattana, C.; Sarasiri, R.; Leyatikul, P. *ASEAN Drug Monitoring Report 2017,* ASEAN Narcotics Cooperation Center: Bangkok, Thailand, 2018.

(10) Cuypers, E.; Bonneure, A. J.; Tytgat, J. *Drug Test. Anal.* **2016**, *8*, 137.

(11) de Jong, M.; Florea, A.; Eliaerts, J.; Van Durme, F.; Samyn, N.; De Wael, K. *Anal. Chem.* **2018**, *90*, 6811.

(12) Deakin, A. *Microgram Journal* **2003**, *1*, 40.

(13) Binette, M.-J.; Pilon, P. *Microgram Journal* **2013**, *10*, 8.

(14) de Jong, M.; Sleegers, N.; Kim, J.; Van Durme, F.; Samyn, N.; Wang, J.; De Wael, K. *Chem. Sci.* **2016**, *7*, 2364.

(15) Rocha, R. G.; Stefano, J. S.; Arantes, I. V. S.; Ribeiro, M.; Santana, M. H. P.; Richter, E. M.; Munoz, R. A. A. *Electroanalysis* **2019**, *31*, 153.

(16) Freitas, J. M.; Ramos, D. L. O.; Sousa, R. M. F.; Paixao, T.; Santana, M. H. P.; Munoz, R. A. A.; Richter, E. M. *Sens. Actuator B-Chem.* **2017**, *243*, 557.

(17) Asturias-Arribas, L.; Alonso-Lomillo, M. A.; Dominguez-Renedo, O.; Arcos-Martinez, M. J. *Anal. Chim. Acta* **2014**, *834*, 30.

(18) Goodchild, S. A.; Hubble, L. J.; Mishra, R. K.; Li, Z. H.; Goud, K. Y.; Barfidokht, A.; Shah, R.; Bagot, K. S.; McIntosh, A. J. S.; Wang, J. *Anal. Chem.* **2019**, *91*, 3747.

(19) Rocha, D. P.; Dornellas, R. M.; Nossol, E.; Richter, E. M.; Silva, S. G.; Santana, M. H. P.; Munoz, R. A. A. *Electroanalysis* **2017**, *29*, 2418.

(20) Shi, H. X.; Xiang, W. W.; Liu, C.; Shi, H. F.; Zhou, Y.; Gao, L. *Nanosci. Nanotechnol. Lett.* **2018**, *10*, 1707.

(21) de Jong, M.; Florea, A.; de Vries, A. M.; van Nuijs, A. L. N.; Covaci, A.; Van Durme, F.; Martins, J. C.; Samyn, N.; De Wael, K. *Anal. Chem.* **2018**, *90*, 5290.

(22) Florea, A.; Cowen, T.; Piletsky, S.; De Wael, K. *Talanta* **2018**, *186*, 362.

(23) Rizvi, M. A. *Russ. J. Gen. Chem.* **2015**, *85*, 959.

(24) Kodama, M.; Murray, R. W. *Anal. Chem.* **1965**, *37*, 1638.

(25) Elgrishi, N.; Rountree, K. J.; McCarthy, B. D.; Rountree, E. S.; Eisenhart, T. T.; Dempsey, J. L. *J. Chem. Educ.* **2018**, *95*, 197.

(26) FernandezAbedul, M. T.; CostaGarcia, A. *Anal. Chim. Acta* **1996**, *328*, 67.

(27) Xi, X.; Ming, L. A.; Liu, J. *Drug Test. Anal.* **2011**, *3*, 182.

(28) Ni, Y. N.; Wang, L.; Kokot, S. *Anal. Chim. Acta* **2001**, *439*, 159.

(29) Chen, Y. L.; Liu, H. H.; Liu, Y. C.; Yang, Z. S. *Anal. Methods* **2014**, *6*, 1203.

For table of contents only